31st Annual International Conference of the IEEE EMBS
Minneapolis, Minnesota, USA, September 2-6, 2009

Investigation on DOT Guided FMT: Whether the FMT Image Quality is Robust to the Priori DOT Information?

Daifa Wang, and Jing Bai*, *Fellow, IEEE*

***Abstract*—The fluorescence molecular tomography (FMT) image quality could be improved significantly with reconstructed optical properties using diffuse optical tomography (DOT). However, different DOT algorithms and different constraint parameters usually lead to DOT images of obvious different image quality. In this paper, simulation experiment results demonstrate that the FMT image quality is robust to the great variation in DOT image quality.**

I. Introduction

In recent years, fluorescence molecular tomography (FMT) has emerged as an important imaging tool for observing molecular function for whole body small animal and entire tissues. The optical imaging tool can quantitatively resolve the fluorescence target distribution, which is corresponding to the molecular function such as protein-protein interaction, drug metabolism, tumor proliferation and apoptosis, etc [1].

The optical properties of small animals and biological tissues are usually heterogeneous. The priori information of tissue optical properties distribution influences the reconstructed fluorescence image quality [2-4]. At present, two strategies are used to handle the heterogeneous optical properties. First, Normalized Born method has been proposed [2], [5], [6] to correct the heterogeneous optical properties influences by dividing the measured fluorescence signals with its corresponding excitation light signals. When using Normalized Born method, the optical properties are assumed homogeneous. Second, the optical properties can be firstly reconstructed using diffuse optical tomography (DOT). The reconstructed optical properties were then used as the priori information for FMT. The reconstructed optical properties in this paper were called the priori DOT information. When using the priori DOT information, Y. Tan *et al.* [3] demonstrated that the reconstructed fluorescence yield was consistent with that obtained using spectroscopic methods. Y. Lin et al. [4] reported that the true fluorophore concentration could be recovered when both the priori structural information and the priori DOT information were utilized. Many other improved FMT images when using the priori DOT information were also reported [7-9].

All the reported results demonstrated that the reconstructed FMT image qualities were improved when using the priori DOT information. However, it should be noted that DOT reconstruction is an ill-posed problem. With the measured excitation signals, the reconstructed DOT images would usually be different when using different reconstruction algorithms. In addition, for the same reconstruction algorithm, different constraint parameters such as the lower and upper bounds of optical properties would lead to different DOT images. Therefore, one problem is whether the different DOT images would lead to great variation of the FMT image quality? In this study, simulation studies were performed to answer this question. Model based iterative image reconstruction scheme (MoBIIR) [10] was used for reconstructing optical properties. Two different optimization algorithms LSQR and MINRES were employed for updating the optical properties in the inner iteration. For each algorithm, two different optical properties lower bounds were set. Therefore, four DOT images with obvious different image contrast were generated from a same set of measured excitation light signals. FMT reconstructions were performed when guided by the four different DOT images. The results demonstrated that the obvious variation in DOT images doesn't lead to obvious variation of the FMT images. Therefore, the FMT image is robust to the priori DOT information.

The outline of this article is presented as follows. In section II, the reconstruction methods are described. Section III describes the simulation experiment and results. Finally, we discuss and conclude our study in section IV.

II. Methods

In the near infrared spectral window, the light propagation in highly scattering tissue media ($\mu_a \ll \mu_s'$) is usually described by the diffusion equation. When excited by a continuous wave point source, the mathematical model for FMT is described by two coupled diffusion equations as follows:

$$\begin{cases} -\nabla\cdot[D_x(r)\nabla\Phi_x(r)] + \mu_{ax}(r)\Phi_x(r) = \delta(r-r_s),\ r\in\Omega \\ -\nabla\cdot[D_m(r)\nabla\Phi_m(r)] + \mu_{am}(r)\Phi_m(r) = \Phi_x(r)n(r),\ r\in\Omega \end{cases}, \quad (1)$$

where subscript x indicates excitation wavelength and subscript m indicates emission wavelength. $\Phi_{x,m}$ is the

Manuscript received April 7, 2009. *Asterisk indicates corresponding author.*

This work was supported by the National Nature Science Foundation of China (No. 30670577, 60831003), the Tsinghua-Yue-Yuen Medical Science Foundation, the National Basic Research Program of China (No. 2006CB705700), the National High-Tech Research and Development Program of China (No. 2006AA020803), and the China Postdoctoral Science Foundation Funded Project.

Daifa Wang and Jing Bai are with Department of Biomedical Engineering, School of Medicine, Tsinghua University, Beijing, 100084, China. (e-mail: deabj@tsinghua.edu.cn).

photon density, $\mu_{ax,am}$ is the absorption coefficient, and $D_{x,m} = 1/(3\mu'_{sx,sm})$ is the diffusion coefficient with $\mu'_{sx,sm}$ as the reduced scattering coefficient. For simplicity, the optical properties at both excitation and emission wavelength are typically assumed the same. $\delta(r - r_s)$ is the point source term at position r_s. A collimated laser source beam can be modeled as an isotropic source which is one transport mean free path $ltr = 3D_x$ beneath the illumination surface. $n(r)$ is the fluorescence yield, which describes the fluorescence target distribution. The diffusion equation is solved by the finite element method.

Absorption optical property is reconstructed before reconstructing the fluorescence target distribution. As shown in Fig. 1, DOT is implemented using the model based iterative image reconstruction scheme [10]. When the media of interest is sampled in voxels, the sensitivity matrix J is calculated using the adjoint method [11]. Then, in each inner iteration, the absorption property is updated using the following equation:

$$(J^T J + \lambda_1 I)\Delta\mu_a = J^T \Delta\Phi_x \quad , \tag{2}$$

where $\Delta\Phi_x$ is the difference between the measured and calculated excitation light photon densities; I is identity matrix; λ_1 is the regulation parameter. Optimization method such as LSQR or MINRES could be used to solve Eq. (2) After implementing the MoBIIR scheme, a line searching method was added to further decrease the mismatch $|\Delta\Phi_x|$ between the measured and the calculated excitation light signals.

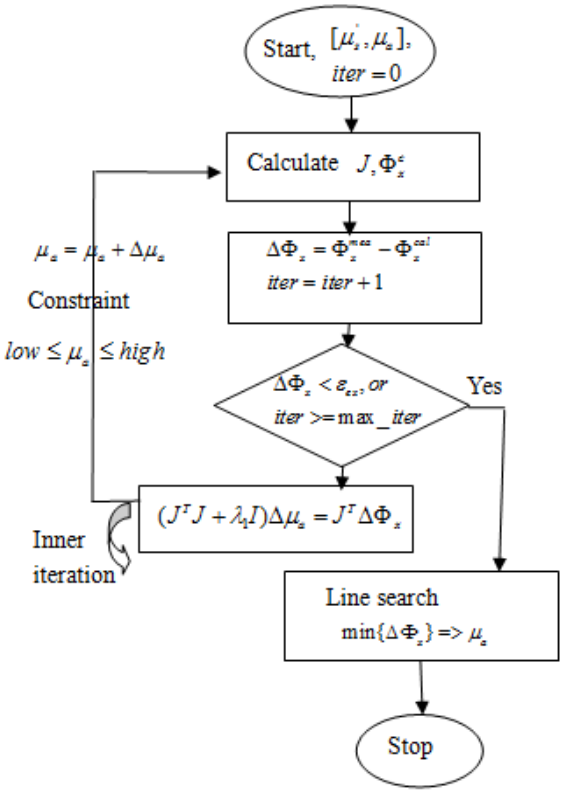

Fig. 1. DOT reconstruction method.

With the knowledge of optical properties, the FMT inverse problem is formulated as follows:

$$(W^T W + \lambda_2 I)n = W^T \Phi_m^{mea} \quad , \tag{3}$$

where Φ_m^{mea} is the measured photon densities at different detector points; W is the sensitivity matrix and is calculated using the adjoint method [11]; λ_2 is the regulation parameter. Gauss-Newton method is used to solve Eq. (3).

III. EXPERIMENT and RESULTS

A. Simulation Experiment

As shown in Fig. 2, the two small black circles of 0.3cm radius represent the absorbers and the fluorescence targets. The optical properties inside the two small circles are $\mu_a = 0.3\text{cm}^{-1}, \mu_s' = 10.0\text{cm}^{-1}$. The background optical properties inside the larger black circle of 1.25cm radius are $\mu_a = 0.1\text{cm}^{-1}, \mu_s' = 10.0\text{cm}^{-1}$. The fluorescence yield is set to 1 inside the two small circles and 0 in the background. 60 sequential illuminated excitation light sources were placed equally at 6-degree step. The detector points are located in $\pm 40^\circ$ field of view of the corresponding light source. The synthetic data were generated using the finite element

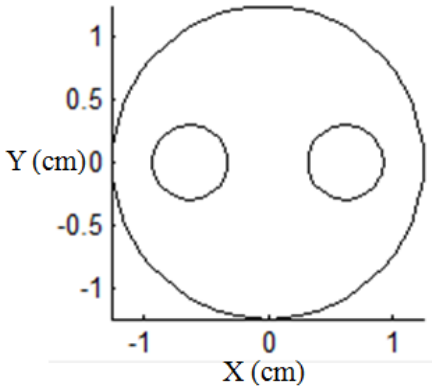

Fig. 2. Simulation experiment setup. The two small black circles represent the absorbers and the fluorescence targets.

TABLE I. Experiment cases.

	case 1	case 2	case 3	case 4
Algorithm	LSQR	LSQR	MINRES	MINRES
lower bound (cm^{-1})	0.1	0.05	0.1	0.05
upper bound (cm^{-1})	0.4	0.4	0.4	0.4

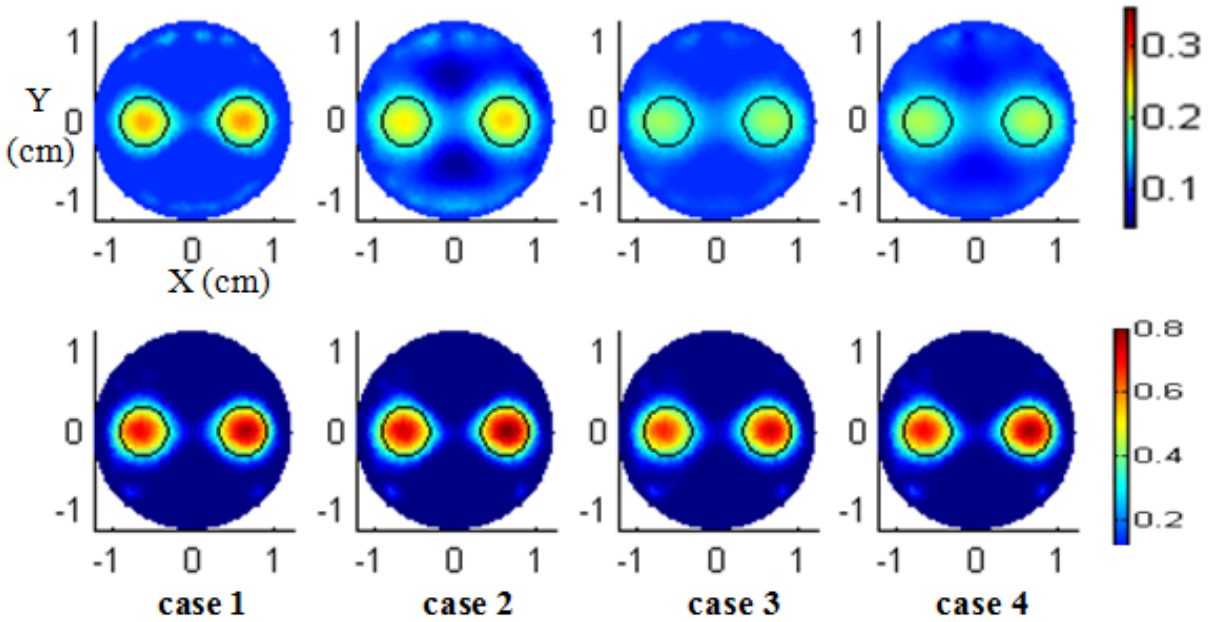

Fig. 3. The reconstructed DOT and FMT images. The images in the first row are DOT images of different cases. The images in the second row are FMT images of different cases.

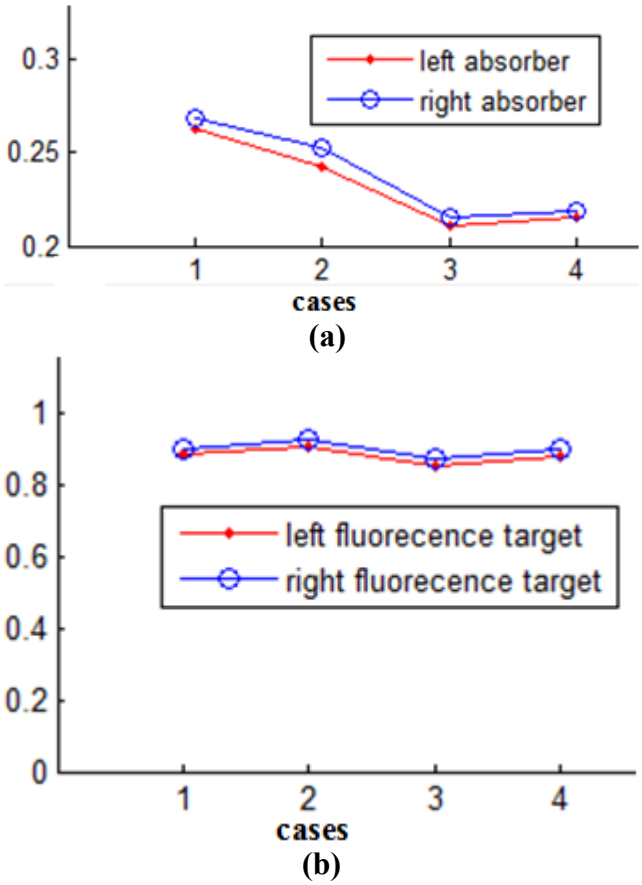

Fig. 4. Statistic results of DOT and DOT guided FMT. (a) The maximum absorption value of the left and right absorbers for the four cases. (b) The accumulated fluorescence yield of the left and right fluorescence targets for the four cases.

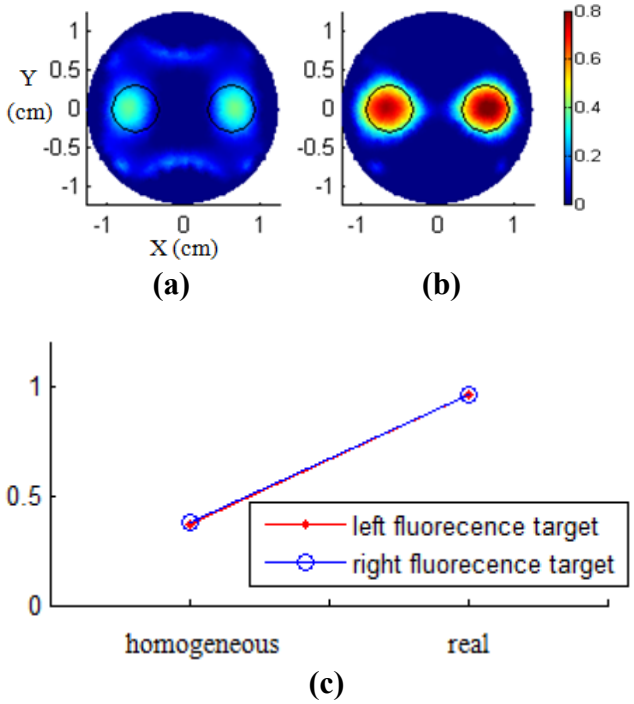

Fig. 5. FMT results with homogeneous and real optical properties. (a) The FMT image assuming homogeneous optical properties. (b) The FMT image assuming real optical properties. (c) The accumulated fluorescence yield.

method.

B. Results

Inner region which is more than 0.1cm away from the outer boundary was selected as the region of reconstruction and sampled into 0.05cmx0.05cm small voxels. DOT images were reconstructed in four cases, as shown in Table I. The lower bound of absorption coefficient was selected close to

the background absorption coefficient. In case 1 and case 2, LSQR was run with 50 iterations. In case 3 and case 4, MINRES was run with 10 iterations. The initial value in all cases was $\mu_a = 0.1\text{cm}^{-1}, \mu_s' = 10.0\text{cm}^{-1}$. The maximum outer iteration number for all cases was set to 5. The regulation parameter of all cases was 2% of the maximum diagonal value of $J^T J$. In FMT image reconstruction, Gauss-Newton method was run with 50 iterations. Non negative constraint was applied. The regulation parameter in all cases was 2% of the maximum diagonal value of $W^T W$. The initial value was set to zero.

The DOT and FMT images of the four cases are shown in Fig. 3. It can be seen that the contrast of the DOT images is of great variation. As shown in Fig. 4(a), the maximum absorption value of the four DOT images varies greatly. In contrary, the image contrast of the FMT images guided by the DOT images doesn't change much. We accumulated the fluorescence yield inside regions which are less than 0.5cm away from the real targets' centers. As shown in Fig. 4(b), the accumulated values are from 85.8% to 90.8% of the real value. Obviously, the accumulated fluorescence yield doesn't change much.

The FMT images with homogeneous ($\mu_a = 0.1\text{cm}^{-1}, \mu_s' = 10.0\text{cm}^{-1}$) and real optical properties are shown in Fig. 5. Obviously, the image quality deteriorates when assuming homogeneous optical properties. At the same time, the reconstructed fluorescence yield assuming homogeneous optical properties were much less that with accurate and the priori DOT information.

IV. Discussion and Conclusion

From the experiment results, we can see that the FMT image quality is improved significantly when using the priori DOT information. At the same time, the FMT image guided by DOT images of obvious different image qualities doesn't change much. Therefore, the FMT image quality is robust to the priori DOT information. It should be also be noted that the accumulated fluorescence yield of the left target using accurate optical properties was about 95.6% of the real value, which are a little more accurate than that with the priori DOT information. That means, if we are able to design a better DOT method leading to a DOT image which approximates real one better, FMT image quality with the priori DOT information still has the potential to be slightly improved. To further validate the conclusions, further investigation will be focused on designing more complex experiment and applying more criterions to evaluating DOT and FMT image qualities.

References

[1] V. Ntziachristos, J. Ripoll, L. V. Wang, and R. Weissleder, "Looking and listening to light: the evolution of whole-body photonic imaging," *Nat. Biotechnol.*, Vol. 23, pp. 313-320, Mar. 2005.

[2] A. Soubret, J. Ripoll, and V. Ntziachristos, "Accuracy of fluorescent tomography in the presence of heterogeneities: study of the normalized born ratio," *IEEE Trans. Med. Imag.*, Vol. 24, pp. 1377-1386, Oct. 2005.

[3] Y. Tan and H. Jiang, "Diffuse optical tomography guided quantitative fluorescence molecular tomography," *Appl. Opt.*, Vol. 47, pp. 2011-2016, Apr. 2008.

[4] Y. Lin, H. Yan, O. Nalcioglu, and G. Gulsen, "Quantitative fluorescence tomography with functional and structural a priori information," *Appl. Opt.*, Vol. 48, pp. 1328-1336, Mar. 2009.

[5] V. Ntziachristos and R. Weissleder, "Experimental three-dimensional fluorescence reconstruction of diffuse media by use of a normalized Born approximation," *Opt. Lett.*, Vol. 26, pp. 893-895, Jun. 2001.

[6] E. E. Graves, J. Ripoll, R. Weissleder, and V. Ntziachristos, "A submillimeter resolution fluorescence molecular imaging system for small animal imaging," Med. Phys., Vol. 30, pp. 901–911, May. 2003.

[7] L. Hervé, A. Koenig, A. Da Silva, M. Berger, J. Boutet, J. M. Dinten, P. Peltié, and P. Rizo, "Noncontact fluorescence diffuse optical tomography off heterogeneous media," *Appl. Opt.*, vol. 46, pp. 4896-4906, 2007.

[8] A. B. Milstein, S. Oh, K. J. Webb, C. A. Bouman, Q. Zhang, D.A. Boas, and R. P. Millane, "Fluorescence optical diffusion tomography," *Appl. Opt.*, vol. 42, pp. 3081–3094, 2003.

[9] D. Wang, X. Liu, Y. Chen, and J. Bai, "A novel finite element based algorithm for fluorescence molecular tomography of heterogeneous media," *IEEE Trans. Inf. Technol. Biomed.* 2009. (Accepted)

[10] A. D. Klose and A. H. Hielscher, "Iterative reconstruction scheme for optical tomography based on the equation of radiative transfer," *Med. Phys.* Vol. 26, pp. 1698-1707, 1999.

[11] S. R. Arridge and M. Schweiger, "Photon-measurement density functions. Part 2: Finite-element-method calculations," *Appl. Opt.* Vol. 34, pp. 8026-8037, Dec. 1995.